The EMBO Journal vol.11 no.9 pp.3203-3208, 1992

X-ray structure of nucleoside diphosphate kinase

Christian Dumas, Ioan Lascu[1], Solange Moréra, Philippe Glaser[2], Roger Fourme[3], Valérie Wallet[1], Marie-Lise Lacombe[1], Michel Véron[1] and Joël Janin

Laboratoire de Biologie Structurale, Bât. 433, UMR 9920 CNRS-Université Paris-Sud, 91405-Orsay, [1]Unité de Biochimie Cellulaire, [2]Unité de Régulation de l'Expression Génétique, (CNRS-URA 1129), Institut Pasteur, 75724 Paris Cedex 15 and [3]LURE, Bât. 209, CNRS-Université Paris-Sud, 91405-Orsay, France

Communicated by J.Janin

The X-ray structure of a point mutant of nucleoside diphosphate kinase (NDP kinase) from *Dictyostelium discoideum* has been determined to 2.2 Å resolution. The enzyme is a hexamer made of identical subunits with a novel mononucleotide binding fold. Each subunit contains an α/β domain with a four stranded, antiparallel β-sheet. The topology is different from adenylate kinase, but identical to the allosteric domain of *Escherichia coli* ATCase regulatory subunits, which bind mononucleotides at an equivalent position. Dimer contacts between NDP kinase subunits within the hexamer are similar to those in ATCase. Trimer contacts involve a large loop of polypeptide chain that bears the site of the Pro → Ser substitution in *Killer of prune* (*K-pn*) mutants of the highly homologous *Drosophila* enzyme. Properties of *Drosophila* NDP kinase, the product of the *awd* developmental gene, and of the human enzyme, the product of the *nm23* genes in tumorigenesis, are discussed in view of the three-dimensional structure and of possible interactions of NDP kinase with other nucleotide binding proteins.

Key words: Dictyostelium discoideum/Drosophila Awd/Nm23/nucleoside diphosphate kinase/X-ray crystallography

Introduction

Nucleoside diphosphate kinase (NDP kinase) exchanges a γ-phosphate between nucleoside tri- and diphosphates: XTP + YDP ⇌ XDP + YTP, through a *ping–pong* mechanism. XTP phosphorylates a histidine, which in turn phosphorylates YDP (Parks and Agarwal, 1973). The enzyme, which is found in all cells, shows little specificity towards the X and Y bases and accepts nucleotides and deoxynucleotides as substrates. Thus, it is the source of most of the RNA and DNA precursors, except ATP.

As a major source of GTP, NDP kinase occupies a central position in the control of cell functions and in development. Eukaryotic NDP kinases have been proposed to interact with heterotrimeric G proteins (Kimura and Shimada, 1990; Wieland *et al.*, 1991; Lacombe and Jakobs, 1992). Gilles *et al.* (1991) have shown that the human NDP kinase is coded by *nm23*, a gene originally characterized as a suppressor of metastasis in a tumour cell line (Steeg *et al.*, 1988). In *Drosophila*, NDP kinase is coded by *awd*, a gene involved in morphogenesis (Dearolf *et al.*, 1988; Rosengard *et al.*, 1989; Biggs *et al.*, 1990). The *Killer of prune* (*K-pn*) mutation (Sturtevant, 1956) is located in *awd* (Dearolf *et al.*, 1988) and substitutes a serine for a proline in *Drosophila* NDP kinase (A.Shearn, personal communication; Lascu *et al.*, 1992). *K-pn* is a dominant lethal mutation (Orevi and Falk, 1975) in flies carrying the *prune* eye colour mutation, which suggests that the product of *awd* interacts with that of *prune*.

We describe here the 2.2 Å resolution X-ray structure of a point mutant of the NDP kinase from the slime mould *Dictyostelium discoideum*, which is highly homologous to the human and *Drosophila* enzymes (Wallet *et al.*, 1990; Gilles *et al.*, 1991). The 100 kDa protein is a symmetrical hexamer. Its subunit structure, novel for a kinase, does not contain the classical mononucleotide binding fold (Schultz, 1992) found in $p21^{ras}$ and in adenylate kinase. Instead, it bears a remarkable similarity to the allosteric domain of *Escherichia coli* aspartate carbamoyltransferase (ATCase), which binds ATP and CTP as NDP kinase does, and at a site close to the putative active site of NDP kinase. The X-ray structure provides a structural interpretation of the *K-pn* mutation, which affects subunit contacts in the hexamer. Reported properties of the human Nm23 protein and possible interactions of NDP kinase with other nucleotide binding proteins are also discussed.

Results and discussion

The H122C mutant protein

Wild type *Dictyostelium* NDP kinase cloned and expressed in *E.coli* (Lacombe *et al.*, 1990), crystallizes in ammonium sulphate, yielding hexagonal crystals with two 17 kDa subunits in the asymmetric unit (Dumas *et al.*, 1991). Due to difficulties in finding heavy atom derivatives in a protein devoid of cysteine, a sulfhydryl group was introduced in the protein by site directed mutagenesis. The target residue was His122, homologous to the residue that has been shown to be phosphorylated during catalysis in human NDP kinase (Gilles *et al.*, 1991). We checked that His122 is phosphorylated in the *Dictyostelium* enzyme (Wallet, 1992).

The H122C protein was expressed with a high yield in *E.coli* as a soluble protein. It was stable and although catalytically inactive, as expected, it could be purified and crystallized under the same conditions as the wild type. It was identical to wild type *Dictyostelium* NDP kinase on the following criteria. The N-terminal sequence was the same, except for the removal of the terminal methionine during expression in *E.coli*. It bound ATP and ADP with dissociation constants of 1 μM and 40 μM respectively, as measured by competition with 2′,3′-trinitrophenyl ADP. Five different monoclonal antibodies raised against the wild type enzyme, two of which inhibit its activity, were

found to react with the H122C protein with affinities similar to the wild type.

The H122C protein gave two distinct crystal forms growing in the same batches. One is isomorphous to wild type crystals, the other belongs to the same hexagonal space group, but the unit cell is smaller and the asymmetric unit contains one 17 kDa subunit rather than two (Table I). These crystals, which diffract to better than 2 Å, were used for this study. Diffraction data were recorded on the wiggler line of LURE-DCI (Orsay) using an image plate system and 0.98 Å synchrotron radiation. Substitution with Hg yielded a single site isomorphous derivative. Owing to the strong anomalous signal of Hg at this wavelength, the electron density map derived from these data was of sufficient quality for most of the polypeptide chain to be traced. Solvent flattening and partial model phasing were applied to improve the map quality. A complete model of the 155 residue long polypeptide chain was built, except for residues 1–7, which were disordered. The present model has an R factor of 20% at 2.2 Å resolution and excellent stereochemistry. A representative part of the electron density map is shown in Figure 1.

The NDP kinase fold

Like other NDP kinases reported so far, the *Dictyostelium* enzyme is a hexamer with $M_r \approx 100$ kDa. It has dihedral three-fold (D3) symmetry—a crystallographic symmetry in this case—as expected for a hexamer. Its shape is compact, ~70 Å in diameter and 50 Å thick (Figure 2). In each 17 kDa subunit, residues 8–138 form a globular α/β domain and residues 139–155, an extended outer segment (Figure 3). The β-sheet is four-stranded, antiparallel and the strand order is 2.3.1.4. Helix α1, connecting β1 to β2, and helix α3, connecting β3 to β4, cover the face of the β-sheet towards the core of the hexamer. The other face of the β-sheet is only partly covered by helix α4 and connecting loops. The active site of the enzyme was marked by Cys122, which replaced the phosphorylated histidine. It belongs to

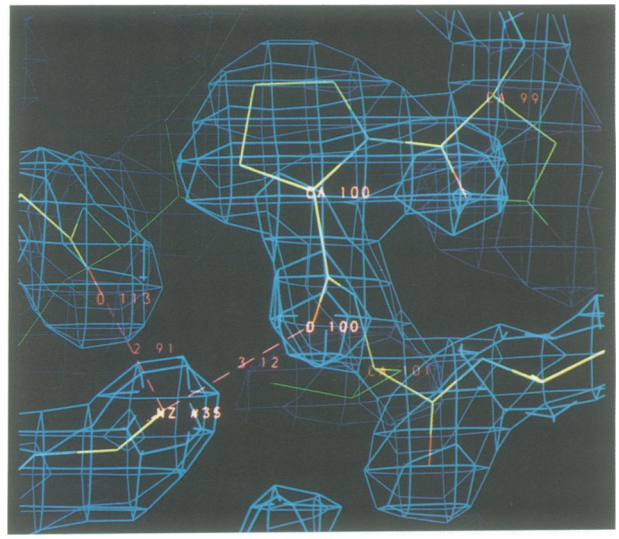

Fig. 1. Electron density near Pro100. Section of the map calculated with $2F_{obs}-F_{calc}$ Fourier coefficients and phases calculated from the current model. The map is contoured at 1σ. Pro100 is equivalent to Pro97 mutated to serine in the *K-pn* mutant of *Drosophila*. Lys35 is from a neighbouring subunit in the hexamer. Its Nζ atom hydrogen bonds to the carbonyl oxygens of Pro100 and Gly113. Drawn with FRODO (Jones, 1985).

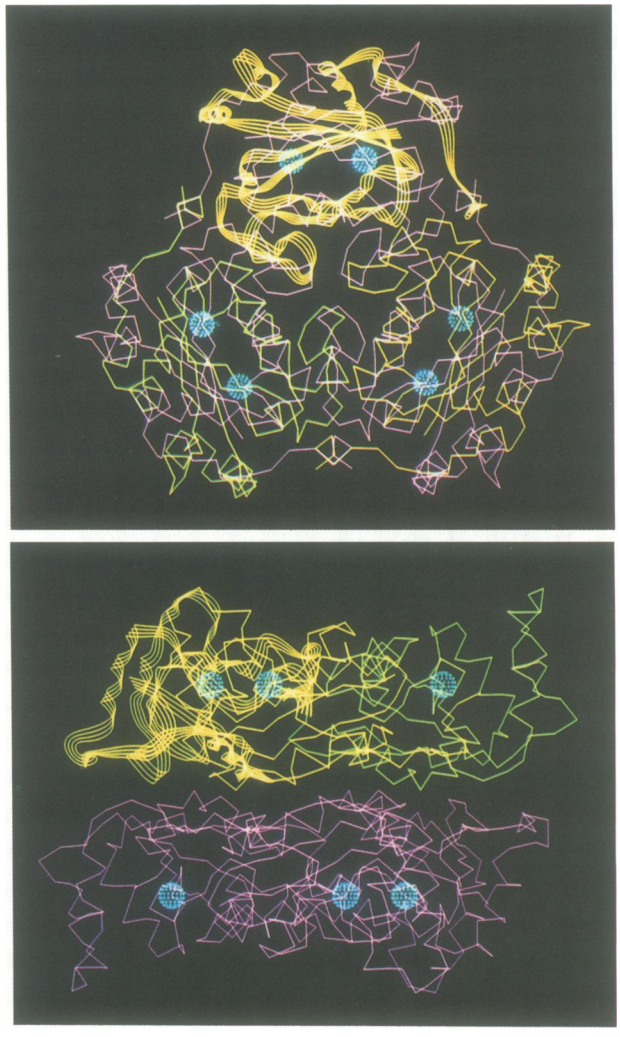

Fig. 2. The *Dictyostelium* NDP kinase hexamer. Views along the three-fold axis (**top**) and in a direction orthogonal to it (**bottom**). Spheres mark the position in each subunit of the active site residue 122, a histidine in wild type enzyme mutated here to a cysteine. Drawn with MANOSK (Cherfils *et al.*, 1988).

Table I. Statistics on crystallographic analysis

	Native[a]	Hg
Diffraction data		
Resolution (Å)	2.2	2.2
Measured intensities	82 562	132 562
Unique reflections	9012	8824
Completeness (%)	99.3	97.1
$<I>/<\sigma I>$	60.5	69.6
R_{merge} (%)[b]	4.6	4.2
Phases		
Resolution limits (Å)	20–2.5	
Mean isomorphous difference (%)	18.4	
Mean anomalous difference (%)	5.5	
r.m.s. F_H/residual	2.6	
r.m.s. F_{ano}/residual	4.1	
Average figure of merit, SIRAS phases	0.72	
Average figure after solvent flattening	0.85	

[a]Crystals are space group $P6_322$, a = b = 72.7 Å, c = 107.5 Å, $\alpha = \beta = 90°$, $\gamma = 120°$, with one 17 kDa subunit per asymmetric unit.

[b]$R_{merge} = \dfrac{\Sigma|I(h)_i - <I(h)>|}{\Sigma <I(h)>}$

strand β4 and its side chain points outwards in a cleft running orthogonal to the β-strands. One edge of the cleft is helix α4, the other, a loop (residues 51−59) inserted between β2 and α2. The cleft is easily accessible from the outside and we have preliminary crystallographic evidence demonstrating that it contains the binding site for nucleotides. Details of the active site are relevant to the wild type enzyme structure to be reported later.

The presence of an α/β domain is a common feature of most kinases. The overall appearance of the NDP kinase subunit is not unlike adenylate and guanylate kinase, which are of comparable size and carry similar reactions. But their mechanism is different, and phosphate transfer from ATP to AMP or GMP is direct rather than through a phosphorylated enzyme intermediate. Adenylate kinase, guanylate kinase and the small GTP-binding protein $p21^{ras}$ contain the classical 'mononucleotide-binding fold', an α/β motif with a parallel β-sheet (Schulz *et al.*, 1986; Schulz, 1992). The NDP kinase fold, which is based on an antiparallel β-sheet, is clearly different. It is nevertheless not uncommon. An examination of recently determined three-dimensional structures shows that the four-stranded β-sheet of NDP kinase and its helix connections are present in the RNA-binding domain of U1 small nuclear ribonucleoprotein A (Nagai *et al.*, 1990), in the activation domain of procarboxypeptidase B (Coll *et al.*, 1991) and in acylphosphatase (Pastore *et al.*, 1992). These proteins are unrelated to each other and to NDP kinase in their amino acid sequence.

An early example of this topology is found in the allosteric domain of *r* (regulatory) subunits of *E.coli* ATCase; *r* subunits form dimers and carry the effector site for ATP and CTP (reviewed in Kantrowitz and Lipscomb, 1988). The suggestion that they are related to NDP kinase was made by Kuo (1991). It is fully supported by the present X-ray structure, although no sequence homology is detected. Figure 4 shows that the structural similarity extends beyond the β-sheet to the nucleotide position, which falls near residue 122 in NDP kinase when the two structures are superimposed, and also to subunit contacts (see below). The α-helices do not superimpose as well and NDP kinase has no equivalent to the second domain of the *r* subunit, which binds a zinc ion.

The NDP kinase subunit, the allosteric domain of ATCase and possibly the RNA-binding domain of the U1 protein, have structural and functional properties in common suggesting that they belong to a novel family of nucleotide binding proteins, of which more examples may be found in the near future.

Subunit contacts and the Kpn loop

Subunits in the NDP kinase hexamer form dimers and trimers. The subunit contacts are extensive and cover 2200 Å^2 per subunit, or 27% of its surface. Dimer contacts, which cover 750 Å^2, involve helix α1 and strand β2 from one subunit running antiparallel to their counterparts in the other subunit (Figure 3b). This type of contact, common in oligomeric α/β proteins, also occurs between the corresponding α-helices and β-strands of the allosteric domain in the *r* subunit dimer. NDP kinase trimer contacts cover 1450 Å^2 per subunit. They involve the extremities of helices α1 and α3, the C-terminal residues 152−155 and a large loop (residues 99−118) connecting helix α3 to strand β4. Loops from three subunits come together at the centre of the trimer and on top of the equivalent region from the other trimer, thus filling the central cavity of the hexamer (Figure 2).

We call loop 99−118 the Kpn loop, as it contains Pro100, which is homologous to the proline residue (Pro97) mutated to a serine in *K-pn* mutants of *Drosophila* (Lascu *et al.*,

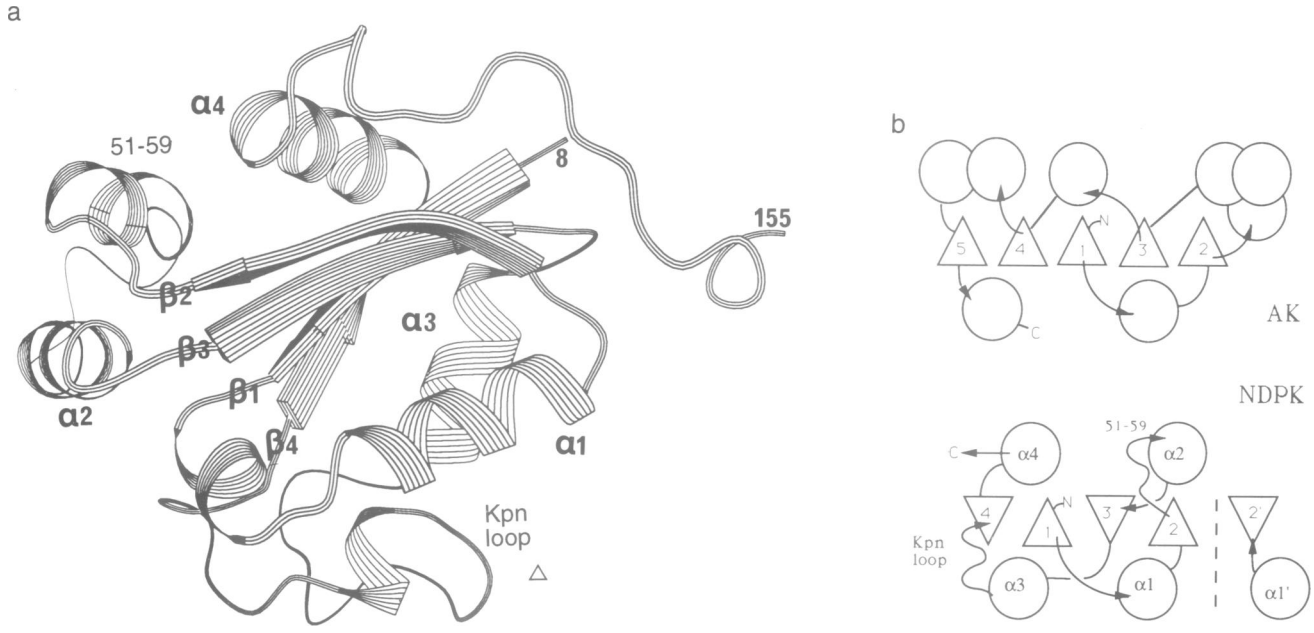

Fig. 3. The NDP kinase fold. (**a**) Ribbon diagram (Priestle, 1988) of the NDP kinase monomer. Residues 1−7 are disordered. The α/β domain (residues 8−138) has a four-stranded antiparallel β-sheet. Strand β4 at the far end carries residue 122 at the active site, which opens towards the top of the figure between helix α4 and loop 51−59 on the left. Loop 51−59, which connects β2 to α2, includes a turn of distorted helix. The C-terminal residues 139−155 form an extended appendix. (**b**) Connectivity diagrams of adenylate kinase and NDP kinase. Triangles pointing up or down are β-strands running in opposite directions. Dashes represent dimer contacts in NDP kinase. The active site cleft is located between loop 51−59 and helix α4.

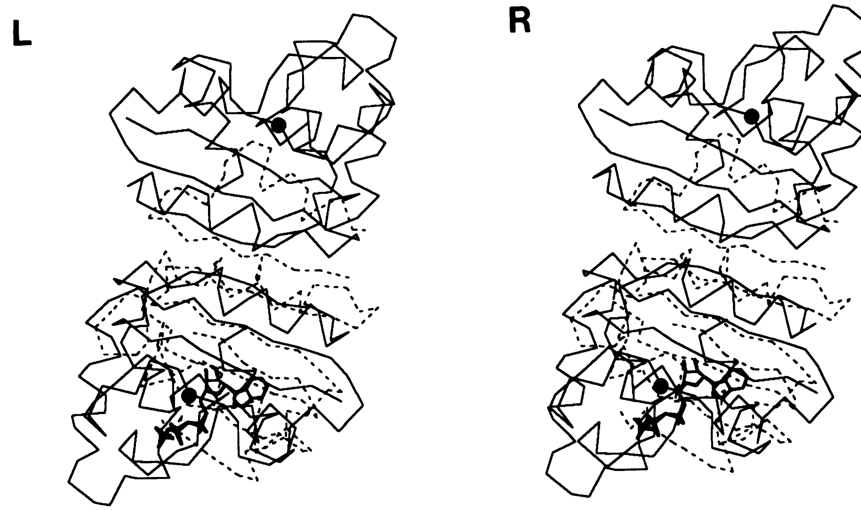

Fig. 4. Comparison with the allosteric domain of *E.coli* ATCase. Stereo diagram of Cα chains in a NDP kinase dimer (residues 8–138, full lines) viewed along its two-fold symmetry axis. The bottom subunit is superimposed with the allosteric domain (residues 8–99, dashes) of the *r* subunit of *E.coli* ATCase complexed with ATP. The nucleotide is drawn with dark bonds. In the H122C mutant protein, the Sγ atom of Cys122 (dot) is 6 Å from the β-phosphate of ATP. The imidazole of His122 in the wild type would be in direct contact. Atomic coordinates for the ATCase–ATP complex (Gouaux *et al.*, 1990) are from Protein Data Bank file 4AT1. A fit based on 40 equivalent Cα atoms yields a r.m.s. distance of 2.4 Å; the β-sheets alone fit to within 1 Å. Part of the second allosteric domain (residues 23–42) in the *r* dimer is drawn to emphasize the similarity in subunit contacts.

```
NDP kinases                  <-β1-->             <---α1--->   <--β2->
                                  10        20        30        40        50
Dictyostelium            MSTNKVNKERTFLAVKPDGVARGLVGEIIARYEKKGFVLVGLKQLVPTKDLAESH
Human A (Nm23-H1)            MA.C....I.I.....Q........K.F.Q...R.....FMQASE..LKE.
Human B (Nm23-H2)            MA.L....I.I.....Q........K.F.Q...R..AM.F.RASEEHLKQ.
Drosophila (Awd)            MAA......IM......Q.....K..E.F.Q...K..A..FTWAS.E.L.K.

                              <--- α2--->  <-β3->     <---α3-->   <--KPN-
                              60        70        80        90        100
Dictyostelium            YAEHKERPFFGGLVSFITSGPVVAMVFEGKGVVASARLMIGVTNPLASAPG
Human A (Nm23-H1)        .VDL.D....A...KYMH........W..LN..KTG.V.L.E...AD.K..
Human B (Nm23-H2)        .IDL.D....P...KYMN........W..LN..KTG.V.L.E...AD.K..
Drosophila (Awd)         ..DLSA....P...NYMN.....P..W..LN..KTG.Q.L.A...AD.L..

                          -- LOOP -->  <β4>  <-- α4---->
                            110       120       130       140       150
Dictyostelium            SIRGDFGVDVGRNII[H]GSDSVESANREIALWFKPEELLTEVKPNPN-LYE
Human A (Nm23-H1)        T.....CIQ......[.]........ EK..G...H....VDYTSCAQ.WI..
Human B (Nm23-H2)        T.....CIQ......[.]......K..EK..S.........VDYKSCAHDWV..
Drosophila (Awd)         T.....CIQ......[.]...A....EK......NEK..V.WTPAAKDWI..
```

Fig. 5. Amino acid sequence and secondary structure assignment. The *Dictyostelium* sequence (Lacombe *et al.*, 1990) is aligned with *Drosophila* Awd (Rosengard *et al.*, 1989) and the human A and B chains (Gilles *et al.*, 1991).

1992; A.Shearn, personal communication). Within the α/β domain (residues 8–138), the *Drosophila* and *Dictyostelium* sequences are 65% identical (Figure 5). This implies very similar tertiary and quaternary structures, with an expected distance between equivalent main chain atoms of <1 Å (Chothia and Lesk, 1986). The sequence homology being high in the Kpn loop, conclusions drawn from the *Dictyostelium* enzyme structure can safely be extended to *Drosophila*. Pro100 is directly implicated in trimer contacts. Its carbonyl group hydrogen bonds to the amino group of Lys35 (Figure 1) from a neighbouring subunit. Both Lys35 and Pro100 are fully buried, and Lys35 is conserved in *Drosophila*. The Kpn NDP kinase is a hexamer, it has normal enzymic activity, but it is less stable towards heat or urea (Lascu *et al.*, 1992). This suggests that the amino acid substitution perturbs the structure of the loop and/or its interactions with neighbouring subunits. *K-pn* is dominant lethal: heterozygous individuals carrying it together with a *prune* mutation die even though they also produce wild type NDP kinase. The sequence of the *prune* gene may be related to that of GTPase activating proteins (Teng *et al.*, 1991). The unusual *K-pn* phenotype cannot be attributed to a loss of enzymic activity or to the relative instability of mutant subunits. Rather, we suggest that in hybrid hexamers mutant subunits can impose a conformation change to wild type subunits through altered contacts between Kpn loops.

The human Nm23 protein

The human NDP kinase has two types of chain, A and B, which readily form hybrid hexamers (Gilles *et al.*, 1991).

The two chains are the product of the genes now called *nm23-H1* and *nm23-H2* (Stahl *et al.*, 1991). They are 88% identical to each other and within the α/β domain they are 67% identical to *Dictyostelium* NDP kinase, again implying that their three-dimensional structures are very similar. Low levels of *nm23-H1* expression have been linked to the increased metastatic potential of some cell lines and tumours (Rosengard *et al.*, 1989; Hennessy *et al.*, 1991; Leone *et al.*, 1991). Yet, the A chain product of *nm23-H1* is overexpressed in highly proliferative cells (Keim *et al.*, 1992) and in a variety of invasive human tumours (Francis *et al.*, 1989; Hailat *et al.*, 1991; Lacombe *et al.*, 1991; Sastre-Gareau *et al.*, 1992). Thus, its role in metastasis control is disputable.

It has been suggested that the Nm23 sequence contains a leucine zipper motif and that NDP kinase is a transcription factor controlling cell proliferation (Stahl *et al.*, 1991). This suggestion is not supported by the three-dimensional structure. The proposed leucine repeat is in a conserved region of the α/β domain, but not in α-helices and the leucine side chains point inwards. If the A chain has a regulatory function other than through nucleotide triphosphate production, it should implicate the few places where its sequence differs from the B chain. Non-conservative substitutions occur at sites equivalent to loop 51–59 and to the C-terminal segment of *Dictyostelium* NDP kinase. Both locations are highly accessible at the protein surface on the periphery of the hexamer. They are plausible candidate sites for interactions of NDP kinase with other nucleotide-binding proteins, which would be responsible for the reported properties of the human enzyme.

Materials and methods

Protein preparation and crystallization

The H122C mutant was prepared by applying the technique described by Kunkel *et al.* (1987) to the *Dictyostelium* gene cloned by Lacombe *et al.* (1990). The following 25mer was used: 5′-GAAACATCATCTGCG-GTTCTGATTC-3′. Mismatched nucleotides are underlined. No additional mutation was found upon resequencing the entire coding sequence.

The mutant protein expressed in *E.coli* was purified following a protocol similar to that reported by Wallet *et al.* (1990) for wild type NDP kinase. The sonicated bacterial extract was centrifuged and the supernatant passed through a DEAE Sephacel column at pH 8.5. This eliminated most of the contaminant proteins, including bacterial NDP kinase. The flow-through was loaded on a Blue Sepharose column. Elution with 1.5 mM ATP yielded a pure H122C protein, as verified by SDS–PAGE. Crystallization was performed in hanging drops over pits containing 2 M ammonium sulphate. The drops contained 5–10 mg/ml protein in 30 mM Tris–HCl, pH 7.2, 1 M ammonium sulphate and 20 mM $MgCl_2$; 1 mM dithiothreitol was added to protect Cys122 from oxidation.

Functional characterization

Nucleotide binding to the H122C protein was measured by competition with 2′,3′-trinitrophenyl ADP. The chromophore was synthesized as described by Hiratsuka and Uchida (1973). Its absorption spectra near 490 nm shifts upon binding to NDP kinase ($\Delta\epsilon_M$ = 3000). Dissociation constants for ADP and ATP were derived as described by Robinson *et al.* (1981). Binding of monoclonal antibodies and their affinity for the H122C protein was measured in solution by the competition method of Friguet *et al.* (1985).

Crystallography

A heavy atom derivative was obtained by co-crystallization of the H122C protein with 5 mM Hg acetate. One native and one derivative crystal, kept at 4°C, were used for data collection. Data extending to 2.2 Å resolution were collected on the W32 station at the LURE-DCI synchrotron (Orsay, France) using a photosensitive plate system. The wavelength was 0.98 Å, near the absorption edge of Hg. With the native crystal, 80° of rotation were recorded about *c* and 30° about a second axis at a rate of 1° per 30 s exposure and per image. Intensities were evaluated with MOSFLM as adapted for the image plate system (Leslie *et al.*, 1986). Further processing using the CCP4 program suite (CCP4, Daresbury Laboratory, Warrington, UK). The Hg position was obvious on both isomorphous and anomalous Patterson difference maps.

A SIRAS map calculated from the Hg position showed the molecular envelope and most of the secondary structure. The map was subjected to solvent flattening (Wang, 1985; Leslie, 1987) and the polypeptide chain was traced with the BONES option of FRODO (Jones, 1985; Jones and Thirup, 1986). After 85% of the side chains were placed in density, calculated phases were combined with the original SIRAS phases using SIGMAA (Read, 1986). Refinement by simulated annealing with X-PLOR (Brünger *et al.*, 1987) reduced the R-factor from 0.42 to 0.26 at 2.5 Å resolution. After minor rebuilding, further X-PLOR refinement was done using only conjugate gradient minimization. The current R-factor is 0.203 for 8697 reflections (99.7% of expected) between 7.0 and 2.2 Å. The current model contains 1118 protein atoms and 28 solvent molecules. RMS deviations from ideal values are 0.010 Å for bond lengths, 1.3° for bond angles, 2.3° for improper dihedral angles (planarity). Only one non-glycine residue, Ile 120, has main chain dihedral angles outside permitted regions of the Ramachandran diagram.

Acknowledgements

We acknowledge the competent assistance of G.Lebras (Orsay) in crystallization. We are grateful to Professor J.P.Benoît and to the staff of LURE (Orsay) for making station W32 on the wiggler line of LURE-DCI available to us, to Dr P.R.E.Evans (Cambridge) and Dr M.Schneider (Martinsried) for the gift of preliminary atomic coordinates of the U1 RNA-binding domain and of procarboxypeptidase B, and to M.Pestel and F.Nato of Hybridolab (Institut Pasteur) for monoclonal antibodies. This work was supported in part by funds from ARC (grant 6438) and the Ligue Nationale Française contre le Cancer.

References

Biggs,J., Hersperger,E., Steeg,P.S., Liotta,L.A. and Shearn,A. (1990) *Cell*, **63**, 933–940.

Brünger,A.T., Kuriyan,J. and Karplus,M. (1987) *Science*, **235**, 458–460.

Cherfils,J., Vaney,M.C., Morize,I., Surcouf,E., Colloch,N. and Mornon,J.P. (1988) *J. Mol. Graphics*, **6**, 155–160.

Chothia,C. and Lesk,A. (1986) *EMBO J.*, **5**, 823–827.

Coll,M., Guasch,A., Avilés,F.X. and Huber,R. (1991) *EMBO J.*, **10**, 1–9.

Dearolf,C.R., Tripoulas,N., Biggs,J. and Shearn,A. (1988) *Dev. Biol.*, **129**, 169–178.

Dumas,C., Lebras,G., Wallet,V., Lacombe,M.-L., Véron,M. and Janin,J. (1991) *J. Mol. Biol.*, **217**, 239–240.

Francis,B., Overmeyer,J., John,W., Marshall,E. and Haley,B. (1989) *Mol. Carcinog.*, **2**, 168–178.

Friguet,B., Chafotte,A.F., Djavadi-Ohaniance,L. and Goldberg,M.E. (1985) *J. Immunol. Methods*, **77**, 305–319.

Gilles,A.M., Presecan,E., Vonica,A. and Lascu,I. (1991) *J. Biol. Chem.*, **266**, 8784–8789.

Gouaux,J.E., Stevens,R.C. and Lipscomb,W.N. (1990) *Biochemistry*, **29**, 7702–7715.

Hailat,N. *et al.* (1991) *J. Clin. Invest.*, **88**, 341–345.

Hennessy,C., Henry,J.A., May,F.E.B., Westley,B.R., Angus,B. and Lennard,T.W.J. (1991) *J. Natl. Cancer Inst.*, **83**, 281–285.

Hiratsuka,T. and Uchida,K. (1973) *Biochim. Biophys. Acta*, **320**, 635–674.

Jones,T.A. (1985) *Methods Enzymol.*, **115**, 252–270.

Jones,T.A. and Thirup,S. (1986) *EMBO J.*, **5**, 819–822.

Kantrowitz,E.R. and Lipscomb,W.N. (1988) *Science*, **241**, 669–674.

Keim,D., Hailat,N., Melhem,R., Zhu,X.X., Lascu,I., Véron,M., Strahler,J. and Hanash,S.M. (1992) *J. Clin. Invest.*, **89**, 919–924.

Kimura,N. and Shimada,N. (1990) *Biochem. Biophys. Res. Commun.*, **168**, 99–106.

Kunkel,T.A., Roberts,O.J. and Zakom,R.H. (1987) *Methods Enzymol.*, **154**, 367–382.

Kuo,L.C. (1991) *Methods Enzymol.*, **202**, 252–270.

Lacombe,M.L. and Jakobs,K.H. (1992) *Trends Pharmacol. Sci.*, **13**, 46–48.

Lacombe,M.L., Wallet,V., Troll,H. and Véron,M. (1990) *J. Biol. Chem.*, **265**, 10012–10018.

Lacombe,M.L., Sastre-Gareau,X., Lascu,I., Wallet,V., Thiéry,J.P. and Véron,M. (1991) *Eur. J. Cancer*, **27**, 1302–1307.

Lascu,I., Chaffotte,A., Limbourg-Bouchon,B. and Véron,M. (1992) *J. Biol. Chem.*, (in press).

Leone,A., Flatow,U., Richter-King,C., Sanden,M., Margoulies,I.M.K., Liotta,L.A. and Steeg,P.S. (1991) *Cell*, **65**, 23–35.
Leslie,A.G.W. (1987) *Acta Crystallogr.*, **A43**, 143–146.
Leslie,A.G.W., Brick,P. and Wonacott,A.T. (1986) *Daresbury Lab. Inf. Quart. Prot. Crystallogr.*, **18**, 33–39.
Nagai,K., Oubridge,C., Jessen,T.H., Li,J. and Evans,P.R.E. (1990) *Nature*, **348**, 515–520.
Orevi,N. and Falk,R. (1975) *Mutat. Res.*, **33**, 193–200.
Parks,R.E., Jr and Agarwal,R.P. (1973) In Boyer,P.D. (ed.), *The Enzymes*, Vol. VIII, pp. 307–334.
Pastore,A., Saudek,V., Ramponi,G. and Williams,R.J.P. (1992) *J. Mol. Biol.*, **224**, 427–440.
Priestle,J.P. (1988) *J. Appl. Crystallogr.*, **21**, 572–576.
Read,R.J. (1986) *Acta Crystallogr.*, **A42**, 140–149.
Robinson,J.B., Brems,D.N. and Stellwagen,E. (1981) *J. Biol. Chem.*, **256**, 10769–10773.
Rosengard,A.M., Krutzsch,H.C., Shearn,A., Biggs,J.R., Barker,E., Margulies,I.M.K., King,C.R., Liotta,L.A. and Steeg,P.S. (1989) *Nature*, **342**, 177–180.
Sastre-Gareau,X., Lacombe,M.L., Jouve,M., Véron,M. and Magdalenat,H. (1992) *Int. J. Cancer*, **50**, 533–538.
Schulz,G.E. (1992) *Curr. Opin. Struct. Biol.*, **2**, 61–67.
Schulz,G.E., Schiltz,E., Tomasselli,A.G., Frank,R., Brune,M., Wittinghofer,A. and Schirmer,R.H. (1986) *Eur. J. Biochem.*, **161**, 127–132.
Stahl,J.A., Leone,A., Rosengard,A.M., Porter,L., King,C.R. and Steeg,P.S. (1991) *Cancer Res.*, **51**, 445–449.
Steeg,P.S., Bevilacqua,G., Kopper,L., Thorgeirsson,U.P., Talmadge,J.E., Liotta,L.A. and Sobel,M.E. (1988) *J. Natl. Cancer Inst.*, **80**, 200–204.
Sturtevant,A.H. (1956) *Genetics*, **41**, 118–123.
Teng,D.H., Engele,C.M. and Venkatesh,T.R. (1991) *Nature*, **353**, 437–440.
Wallet,V. (1992) PhD Thesis, Université Paris 6, Paris.
Wallet,V., Mutzle,R., Troll,H., Barzu,O., Wurster,B., Véron,M. and Lacombe,M.-L. (1990) *J. Natl. Cancer Inst.*, **82**, 1199–1202.
Wang,B.C. (1985) *Methods Enzymol.*, **115**, 90–112.
Wieland,T., Bremerich,J., Bremerich,P. and Jakobs,K.H. (1991) *Eur. J. Pharmacol.*, **208**, 17–23.

Received on April 13, 1992; revised on May 29, 1992